Mechanism for the Excitation of Myocardial Tissue: Results Based on a Three-Dimensional Numerical Model

D. MÜSSIG, B. HENSEL
Department of Biomedical Engineering, Friedrich-Alexander University Erlangen-Nuremberg, Erlangen, Germany

Summary

This paper discusses a mathematical approach to the simulation of atrial myocardial tissue and the interaction with external electrical fields, such as the stimulation pulse of a cardiac pacemaker. The mathematical tissue model is based on the model of an adult human atrial cell. The integration of this model into two interconnected, three-dimensional electrical networks leads to a system of differential equations that is solved in two steps. First, the differential equations of the membrane patch are solved using the Runge-Kutta integration method 4th order; in the second step, the electrical potential of the matrix notes are approximated by the conjugate gradients method. The conduction velocity of the excitation wave could be adjusted by the use of the gap-junction conductance, the only free system parameter. Using this model makes it possible to generate an excitation wave by applying a pacing pulse, and also study the behavior of the membrane channels. The excitation threshold of the model shows a chronaxie-rheobase relationship that could not be shown if a current were injected directly into an isolated cell. This model enables us to study the interaction between myocardial tissue and alternating currents to further understand the ablation process, and helps us to comprehend the mechanism of atrial flutter and fibrillation and the development of concepts for their termination.

Key Words

Stimulation, myocardial tissue, numerical model

Introduction

The influence of external electrical fields on myocardial tissue is difficult to investigate in-vivo because of the excitation mechanism followed by the contraction of the tissue when the electrical threshold is reached. This property of myocardial tissue is well-known and is used in implantable devices for the electrostimulation of the heart. New approaches for the treatment of atrial fibrillation or congestive heart failure using implantable pacemakers are currently being investigated. To reach this goal, multi-chamber devices are being developed to also stimulate the left side of the heart. However, the clinical success of these approaches is determined based on the theoretical understanding of the interaction of multiple excitations and contraction waves, as well as adjustments to the timing of the stimulation. There are many scientific papers describing the different types of myocardial cells available [1-4], but only a few articles could be found describing myocardial tissue [5-7]. Based on this information, an atrial tissue model was developed to investigate the interactions between external electrical currents and myocardial tissue at the microscopic level.

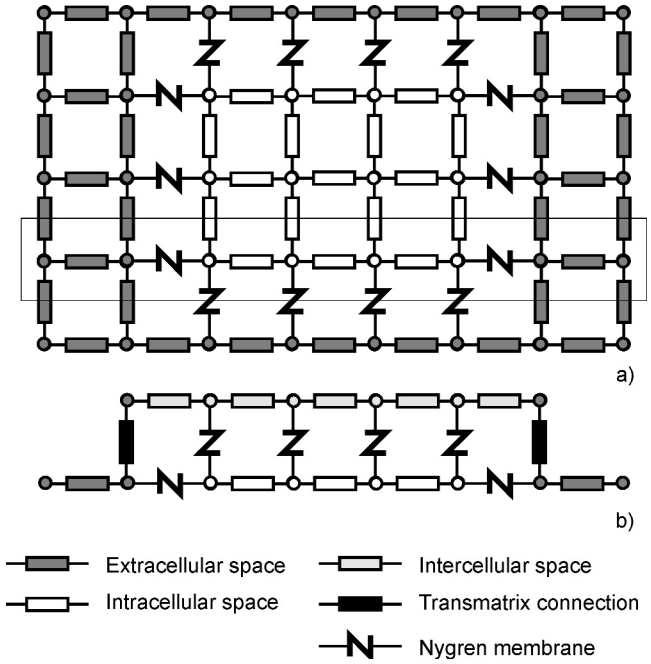

Figure 1. Illustration of the resistor network.
Panel a) Cut in the xy-level; membrane patches separate the extracellular space and the intracellular space.
Panel b) Cut in the tissue-cleft space-level (bordered area in panel a). Every intracellular node is connected to the cleft space via a membrane patch. The matrices are coupled via transmatrix connections.

Materials and Methods

The atrial tissue model is based on an adult human atrial cell model published by Nygren et al. [8]. The model contains six time-dependent ion channels:

- I_{Na} sodium inward current,
- I_{CaL} calcium inward current,
- I_t transient potassium outward current,
- I_{sus} sustained potassium outward current,
- I_{Kr} rapid potassium outward current,
- I_{Ks} slow potassium outward current;

and

- I_{K1} potential-dependent potassium inward current
- I_{CaP} calcium-pump,
- I_{NaK} sodium-potassium pump,
- I_{Na-Ca} sodium-calcium exchange current,
- I_{BNa} sodium leakage current, and
- I_{BCa} calcium leakage current.

For a complete description of the behavior inside the cell, the membrane model is coupled with a fluid compartment model that includes ion-concentration changes in the sarcoplasmic reticulum as well as the extracellular space. The changes of the transmembrane potential are calculated corresponding to the Hodgkin-Huxley formalism ($dV/dt = -I_{membrane}/C_{membrane}$).
The mechanism of coupling cells to myocardial tissue is most important in describing the properties of myocardial tissue. The basic assumption of the developed tissue model is that for every node of the network, Kirchhoff's law is effective. The model consists of a three-dimensional matrix of nodes. The specific potential, e.g., the potential of the extracellular space, the intracellular space, or the potential of the stimulating electrodes is linked to every node of the matrix. Resistors using the extracellular medium as the conductor connect the nodes of the extracellular space. Every intracellular node represents a Nygren cell. In the case of the neighboring extracellular node, a membrane patch connects both nodes. A resistance network that reflects the electrical connection via gap-junction connects the intracellular nodes. It must be noted that all given values of gap-junction conductivity in this article are the mean conductivity of the intracellular space and the cell connecting gap-junction. Because the excitation velocity is two to three times higher along the myocardial fiber compared to the transverse direction, different conductivities are applied in the x, y, and z direction [9]. Parallel to the gap-junction network, every intracellular node is connected to the cleft space via a membrane patch. Again, the cleft space has an electrical connection to the extracellular space. The model is designed to have non-flux conditions at the borders. In Figure 1, the matrix array is schematically shown in a simplified, two-dimensional space.
The equation system is achieved in two steps. In the first step the use of the 4^{th} order Runge-Kutta method with adaptive increment solves the differential equations of the membrane patches. The received potentials of the nodes compose a linear system of equations that is approximated by the conjugate gradient method [10]. In the presented model the method is continued until the error is less 10^{-20}.

Results

The implementation of the cell model into the three-dimensional tissue model leads to new free parameters such as conductivity of the gap-junction, the conductivity of the cleft space, and the extracellular space.

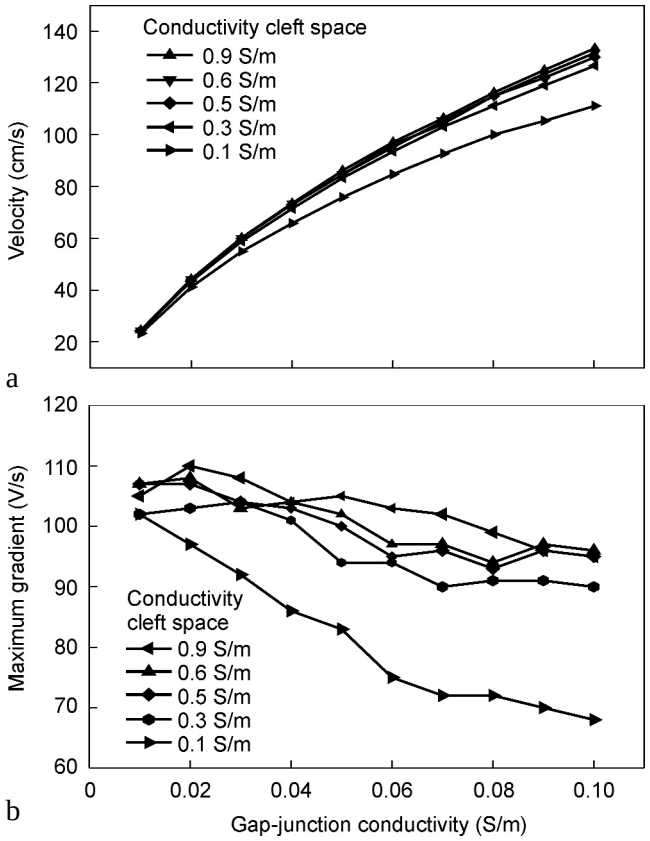

Figure 2. Conduction velocity (panel a) and maximum depolarization gradient (panel b) are dependent of the gap-junction conductivity for different conductivities of the cleft space.

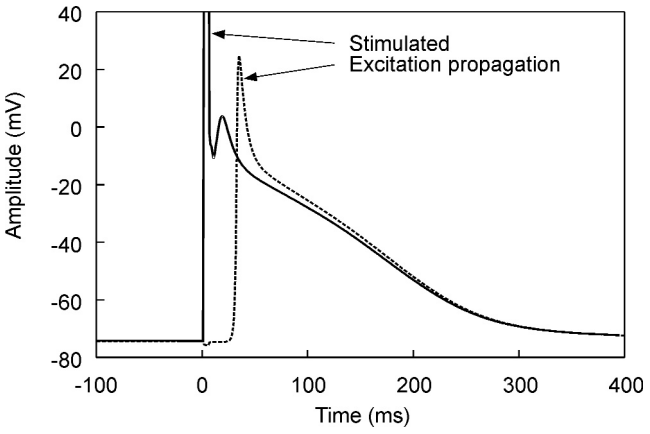

Figure 3. Morphology of the simulated action potentials; the continuous line shows the direct stimulated action potential, the dashed line shows the action potential generated by the excitation wave.

These parameters have a strong influence on the behavior of the tissue. All parameters used in the system, except for gap-junction conductivity, are based on experimental data found in the literature [7,11,12].

Conduction Velocity

For determining the conduction velocity dependency on the gap-junction conductivity, a system containing 12288 nodes has been generated. The embedded tissue consists of 5084 extracellular and 988 intracellular nodes, 640 cleft connections and 640 membrane patches to the extracellular space, as well as 1024 membrane patches to the cleft space. An electrode is placed inside the base of the tissue. By increasing the membrane potential of the point to 0 mV an excitation wave is generated that uniformly spreads out into the z-direction of the tissue. Two measurement electrodes located in the longitudinal direction of the tissue detect the excitation wave. The conduction velocity and maximum depolarization gradient can be analyzed based on the timing information and the morphology of the membrane potential. Because of the use of such a large system, disturbing border effects could be eliminated.

In Figure 2a, for different conductivities of the cleft space the behavior of the conduction velocity is shown; it is dependent on the gap-junction conductivity. For all variations shown, the curve of the conduction velocity is the expected root-dependency; it varies between 23 cm/s at a gap-junction conductivity of 0.01 S/m, up to 133 cm/s at a gap-junction conductivity of 0.1 S/m. The influence of the cleft space conductivity to the conduction velocity is only significant for a very small value of 0.1 S/m. This behavior is due to a disproportionate conductivity between the gap-junction and the cleft space. Figure 2b shows the corresponding maximum depolarization gradient. For cleft space conductivities larger than 0.3 S/m it reaches a value of about 110 V/s at a gap-junction conductivity of 0.02 S/m. The increase of the gap-junction conductivity will result in a slightly decrease of the maximum dipolarization gradient to 90 V/s. This decrease is due to the maceration of the excitation wave at higher conductivities.

Stimulation with DC-Pulses

For analysis of the stimulation mechanism with pacemaker-like DC-pulses, an $11 \times 24 \times 2$ mm^3 tissue piece integrated into a $15 \times 30 \times 13$ mm^3 system was used. The gap-junction conductivity was adjusted in order to achieve a conduction velocity of 70 cm/s and a corre-

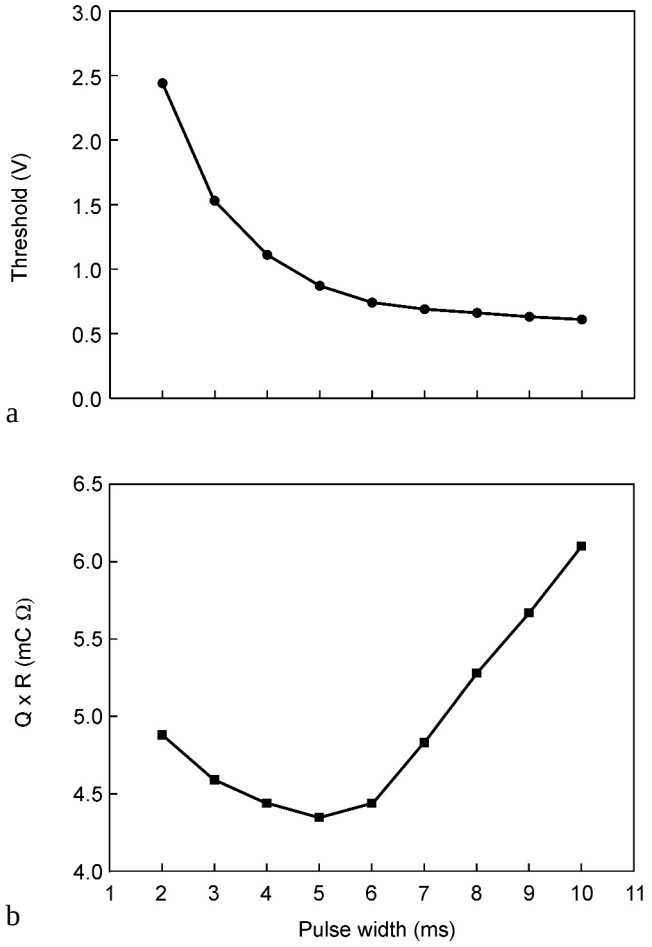

Figure 4. Threshold behavior of the tissue model. Panel a) Electrical threshold at different pulse durations. Panel b) Charge transferred over the electrode at an effective stimulation.

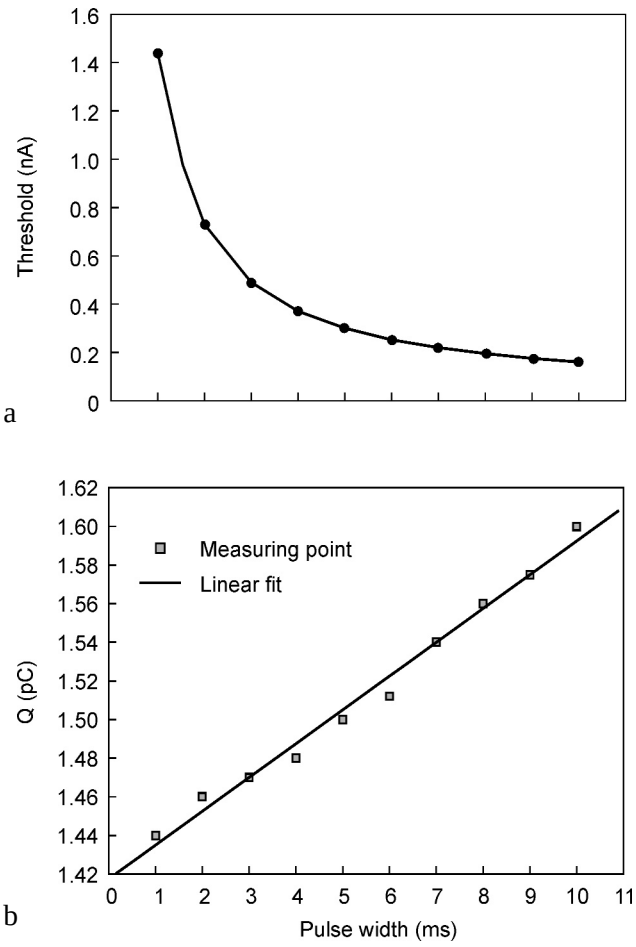

Figure 5. Threshold behavior of an isolated cell. Current that is applied directly into the cell by a micropipette (panel a) and transferred charge Q (panel b).

sponding maximum depolarization gradient of about 100 V/s. The different stimulation electrode was placed 1 mm from the tissue surface, and the indifferent electrode was located 2 mm behind the different electrode. The cell properties were analyzed using measurement points located directly under the different electrode and at a 15 mm distance in the lateral direction. Figure 3 shows the resulting action potential of the measurement points. The stimulation was achieved by applying a DC-pulse of 5 ms duration and an amplitude of −1000 mV. Comparison of the signal morphology shows differences especially in the depolarization phase of the signals. In order for the direct stimulated action potential to show a strong incision after the stimulation artifact, the total duration is prolonged by 25 ms. The signal generated by the excitation wave at the second measurement point shows the identical morphology to the action potential published by Nygren [8].

The electrical threshold of the heart depends on the duration of the applied pulse. This behavior is known as the chronaxie-rheobase relationship. Figure 4a shows the threshold pulse duration dependency of the tissue model. As expected, the increased pulse duration decreases the threshold. Using a 2 ms pulse duration, a 2.44 V pulse amplitude is necessary to generate an excitation wave. This value is decreased to 0.66 V at an 8 ms pulse duration. A further increase of the pulse duration does not lead to a significant decrease of the threshold; e.g., at a 10 ms pulse duration the deter-

mined threshold was 0.61 V. Taking into consideration the charge that is transferred over the electrode at a constant resistance, a minimum could be found (see Figure 4b). This minimum is located close to the chronaxie and corresponds to the minimal energy that is necessary to stimulate the heart using an implantable device. The behavior of the electrical threshold of an isolated cell in the Nygren-model is shown in Figure 5a. In this simulation, in addition to the transmembrane currents (I_{ion}), a current (I_{stim}) is directly applied by a micropipette inside the cell ($dV/dt = -\{I_{ion} + I_{stim}\} / C_{membrane}$). This current leads to an increase in the membrane potential followed by excitation of the cell. As expected, the electrical threshold of the cell decreases with an increased pulse duration (1440 pA at 1 ms to 160 pA at 10 ms). In contrast to the tissue model, the isolated cell model shows no chronaxie-rheobase relationship; the behavior could be approximated by a hyperbolic function. Integration of this function leads to the charge that is necessary to effectively stimulate the cell (Figure 5a). The analysis leads to a linear function charge Q (pC) = A + B × pulse width (ms) with the parameters A = 1.417 ± 0.004 and B = 0.0175 ± 0.0007. In the case of an infinitely short pacing pulse, a charge of 1.417 pC has to be transferred into the cell to excite the cell. Every millisecond the cell itself is able to move a charge of 0.017 pC.

Conclusion

By integrating the cell model of an adult human atrial cell into a three-dimensional network, it is possible to simulate the electrical behavior of the human myocardium. All necessary parameters of the model, except the conductivity of the gap-junction, are based on physiologic examinations found in the literature. The experimental adjustment of the gap-junction conductivity resulted in a system in which the conduction velocity as well as the maximum depolarization gradient was comparable to the human atrial myocardium. The integration of the tissue model into an extracellular space facilitated the stimulation with pacemaker-like pulses. Using field stimulation the tissue model showed the well-known chronaxie-rheobase relationship, in contrast to stimulation by injecting a current directly into an isolated cell. Based on this model, further investigations will be conducted to examine the interaction of electrical currents and human myocardium on the microscopic level.

References

[1] Bristow DG, Clark JW. A mathematical model of primary pacemaking cell in SA node of the heart. Am J Physiol. 1982; 243: H207-H218.

[2] Courtamanche M, Ramirez RJ, Nattel S. Ionic mechanisms underlying human atrial action potential properties: Insights from a mathematical model. Am J Physiol. 1998; 275: H301-H321.

[3] Demir SS, Clark JW, Murphey CR, et al. A mathematical model of a rabbit sinoatrial node cell. Am J Physiol. 1994; 266: C832-C852.

[4] Luo C, Rudy Y. A dynamic model of the cardiac ventricular action potential. Cardiovasc Res. 1994; 74: 1071-1096.

[5] Cartee LA, Plonsey R. Active response of a one-dimensional cardiac model with gap-junctions to extracellular stimulation. Med Biol Eng Comput. 1992; 30: 389-398.

[6] Henriquez CS. Simulating the electrical behavior of cardiac tissue using the bidomain model. Crit Rev Biomed Eng. 1993; 21: 1-77.

[7] Nygren A, Giles WR. Mathematical simulation of slowing of cardiac conduction velocity by elevated extracellular [K^+] in a human atrial strand. Ann Biomed Eng. 2000; 28: 951-957.

[8] Nygren A, Fiset C, Firek L, et al. Mathematical model of an adult human atrial cell: The role of K^+ currents in repolarization. Circ Res. 1998; 82: 63-81.

[9] Spach MS, Francis Heidlage J, Dolber PC, et al. Electrophysiological effects of remodeling cardiac gap-junctions and cell size. Circ Res. 2000; 86: 302-311.

[10] Press WH, Teukolsky SA, Vetterlin WT, et al. Numerical Recipes in C: The Art of Scientific Computing. Cambridge: Cambridge Academic Press. 1992.

[11] Nygren A, Clark RB, Belke DD, et al. Voltage-sensitive dye mapping of activation and conduction in adult mouse hearts. Ann Biomed Eng. 2000; 28: 958-967.

[12] Nygren A, Halter JA. A general approach to modeling conduction and concentration dynamics in excitable cells of concentric cylindrical geometry. J Theor Biol. 1999; 199: 329-358.

Contact
Dr. Dirk Müssig
Department of Biomedical Engineering
Friedrich-Alexander-University
Erlangen-Nürnberg
Turnstrasse 5
D-91054 Erlangen
Germany
Fax: +49 9131 27196
E-mail: dmuessig@biomed.uni-erlangen.de